

Further study of (μ, π) and (μ, γ) invariant masses

C. A. Ramm

University of Melbourne, Parkville, Victoria, Australia 3052

(Received 28 December 1981)

The investigation of neutral (μ, π) invariant masses ($M_{\mu\pi}$) from ν_μ interactions with nucleons and from the decay $K_L^0 \rightarrow (\mu, \pi, \nu)$ has been continued. The phenomena which the author considers to be due to the decay of a short-lived neutral heavy lepton, $M_{\mu\pi}^* \rightarrow (\mu, \pi)$, of mass 0.429 ± 0.002 GeV are found again in new observations of ν_μ interactions. So also are phenomena which are attributed to the decay of a short-lived heavy muon, $M_{\mu\gamma}^* \rightarrow (\mu, \gamma)$, with a mass within ± 0.010 GeV of $M_{\mu\pi}^*(0.429)$. Methods of analysis and searches for errors are described. The invariant-mass distributions from different experiments are compared.

I. INTRODUCTION

ν experiments in the 1.1-m³ version of the CERN heavy-liquid bubble chamber (HLBC) produced 251 interactions of the type

$$\nu_\mu + N \rightarrow \mu^- + \pi^+ + \cdots + N', \quad (1)$$

and 12 of the type

$$\bar{\nu}_\mu + N \rightarrow \mu^+ + \pi^- + \cdots + N', \quad (2)$$

with only one possible neutral combination of (μ, π) ; N is a nucleon in propane (C₃H₈). Although it was expected that the phase space of (μ, π) invariant masses ($M_{\mu\pi}$) would be smooth, it was seen that the largest fluctuation in the observed distribution resembled a similar fluctuation in $M_{\mu\pi}$ distributions from the decay $K_L^0 \rightarrow (\mu, \pi, \nu)$ also expected to be smooth. Each of these features was contributed to by (μ^-, π^+) and (μ^+, π^-) .

Investigation showed that it was extremely unlikely that the coincidence of enhancements was due to statistical fluctuations. The angular distribution of the μ in the (μ, π) center-of-mass systems (c.m.s.) in the enhancements was different from neighboring regions of $M_{\mu\pi}$. No tenable explanation of the observations as errors in experiments or the analyses, or as a known phenomenon, could be proposed at that time, nor since: they are compatible with the proposition that in the interactions of ν_μ and $\bar{\nu}_\mu$ with nucleons, and in K_L^0 decay, neutral particles^{1,2} are produced, and then decay rapidly: $M_{\mu\pi}^* \rightarrow (\mu^-, \pi^+)$ and $\bar{M}_{\mu\pi}^* \rightarrow (\mu^+, \pi^-)$. A mass of 0.429 ± 0.002 GeV for $M_{\mu\pi}^*$ was determined from the K_L^0 data, where the mean absolute errors were < 0.002 GeV.

There has been no independent confirmation of

this proposition: it was refuted soon afterwards by reports^{3,4} that in prolific $M_{\mu\pi}$ distributions from some K_L^0 -decay configurations there were no significant enhancements at or near 0.429 GeV.

The ν experiments in propane and in freon (CF₃Br) in the heavy-liquid bubble chamber, Gargamelle, presented the first possibility to reexamine my analyses in more ν interactions than from the HLBC. I am deeply grateful for access to the Gargamelle data-summary tapes (DST).

This paper describes my own investigations with the aim that they can be tested in other studies; it does not implicate the views of any members of the experimental groups who made their observations available to me. It will be seen that the results of the earlier analyses are reproduced in their entirety in the information on the DST, giving further independent evidence of the decay of $M_{\mu\pi}^*(0.429)$ and also of the charged particle: $M_{\mu\gamma}^* \rightarrow (\mu, \gamma)$, of similar mass.

II. CALIBRATION OF INVARIANT MASSES

Unconstrained invariant masses in the HLBC were calibrated¹ from the weighted mean mass of seven two-prong events likely to be $\Lambda^0 \rightarrow (\pi^-, p)$. Because $m_\mu \sim m_\pi \ll m_p$, it is evident that for (μ, π) and (π, π) of similar momenta, the decays $K_S^0 \rightarrow (\pi, \pi)$ are a better reference than $\Lambda^0 \rightarrow (\pi, p)$ for the calibration of $M_{\mu\pi}$ scales near 0.429 GeV. There is no group of (π, π) from the HLBC identifiable as K_S^0 decays: there is on the DST.

Figure 1 shows histograms of the range 0.380 $< M_{\mu\pi} < 0.570$ GeV as calculated from all two-prong events permitting a (π^+, π^-) hypothesis.

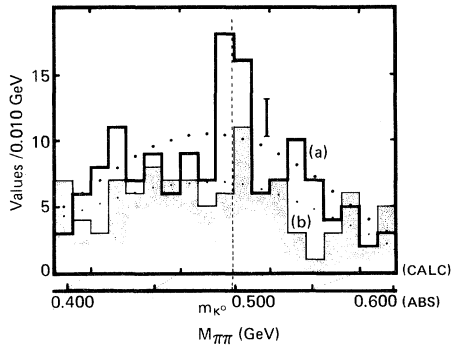


FIG. 1. Histograms of $M_{\pi\pi}$ from events on the DST selected for a (π^+, π^-) hypothesis; the events for (a) are such that the first π read from the DST has $t < 60^\circ$, (b) is from the rest of the events. The dotted lines are least-squares-fitted polynomial means. The scale indicated as (CALC) refers to the edges of the bins of $M_{\pi\pi}$ as calculated; the absolute scale (ABS) is made on the assumption that the mean value of $M_{\pi\pi}$ in the enhancement in (a) is m_{K^0} .

An empirical selection has been developed, independent of particle energy, which enhances the effect likely to be due to K_S^0 . The x direction for the DST is that of the ν beam, along the axis of the cylindrical chamber of Gargamelle; the (y, z) plane is vertical, the optical axes of the cameras are symmetrically disposed about the (z, x) plane. Suppose p_y, p_z are (y, z) components of momentum of the first π of each (π, π) as read from the DST. The selection is that the $M_{\pi\pi}$ of those (π, π) for which $t = \tan^{-1} |p_z/p_y| < 60^\circ$ are in histogram (a); those $M_{\pi\pi}$ for which $t > 60^\circ$ are in (b). The choice of 45° instead of 60° does not change significantly the difference in enhancements in the histograms.

No calculated phase space is available for the histograms in this paper, therefore a least-squares-fitted fourth-degree-polynomial mean of all bins has been plotted in each as an objective reference. Typically, the fourth is the lowest degree which is convenient: in histograms of ~ 25 bins, a polynomial mean is not seen to follow coherent fluctuations over two or three bins until it is about the tenth degree.

The probability that the excess in (a) in the bins $0.470 < M_{\pi\pi} < 0.490$ GeV might be a statistical fluctuation in an observed distribution for which the means are the expected values is $< 3 \times 10^{-3}$; for the excess in the bin $0.480 < M_{\pi\pi} < 0.490$ in (b) it is ~ 0.1 . Because there is some K_S^0 production in the ν interactions, it is likely that the enhancement in (a) is due to decays of K_S^0 in which the

(π, π) are well measurable. The difference between (a) and (b) may be due to the dispositions of the cameras and the magnetic field: on average, tracks of the π 's of (a) may be better identified and more precisely measurable than those of (b).

According to the location of the enhancement in (a) the unconstrained $M_{\pi\pi}$ near m_{K^0} are, on average, 0.019 ± 0.004 GeV lower than the absolute values; their spread is contained within ± 0.010 GeV, which is taken as indicative of the experimental resolution in the DST. No attempt has been made to correct the individual calculated $M_{\pi\pi}$; instead an absolute scale for the bin edges in Fig. 1 has been made, assuming small systematic errors proportional on average to the Q value, i.e., to $M_{\pi\pi} - 2m_\pi$. Therefore, while the contents of the bins are unchanged, their widths in absolute mass vary slightly across the histogram. A similar calibration according to Q value, $M_{\mu\pi} - m_\mu - m_\pi$, will be made for the bin edges of the $M_{\mu\pi}$ histograms. The selection $t < 60^\circ$ will be made also in the μ momenta from the DST because it enhances the effects attributed to $M_{\mu\pi}^*$ near 0.429 GeV in the same way as for the effects attributed to K_S^0 .

III. $M_{\mu\pi}$ FROM ν EXPERIMENTS

Not all individual tracks of μ and π in the ν experiments can be identified with certainty; however, according to their average characteristics, the

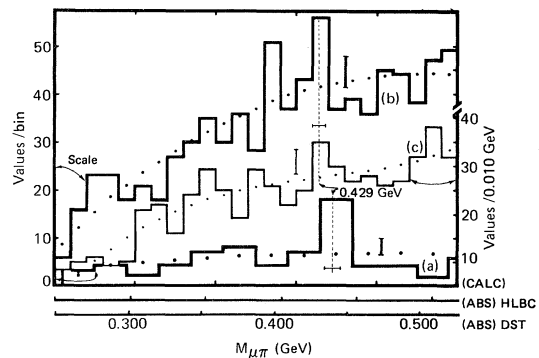


FIG. 2. Histograms of $M_{\mu\pi}$ from ν_{μ} and $\bar{\nu}_{\mu}$ interactions with nucleons; (a) is from the HLBC, reported previously (bins 0.020 GeV); (b) is from events on the DST with only one possible neutral (μ, π) , (bins 0.010 GeV); (c) is from events with one μ and either two or three possible values of $M_{\mu\pi}$. The calculated mass scale refers to unconstrained $M_{\mu\pi}$. The absolute scales are made by reference to Λ^0 decays (HLBC) and the K_S^0 decays in Fig. 1 (DST); the dashed lines are at 0.429 GeV, absolute, in each histogram.

assignments must be mostly correct. The events selected from the DST are inside the fiducial volume and have "one good muon", i.e., each has one track assigned as μ and no other as likely to be μ ; it is required that the "visible" $\sum p_x > 0.3$ GeV/c.

Histogram (a) in Fig. 2 contains 70 $M_{\mu\pi}$ from (μ, π) in event types (1,2) with one identified π from the HLBC.¹ Histogram (b) contains 835 $M_{\mu\pi}$ for events in which only one track accords with a π hypothesis for the DST. (c) is for events on the DST in which either two or three tracks could be π of charge opposite to the μ and which yield, therefore, two or three $M_{\mu\pi}$: there are 578 values.

According to earlier studies, I would expect the largest excess above the mean in (b) to be centered at an absolute mass of 0.429 ± 0.002 GeV. As can be seen, the bin with the largest excess covers the range of calculated masses $0.410 < M_{\mu\pi} < 0.420$ GeV. If the correction for the calculated $M_{\pi\pi}$ near m_{K^0} in Fig. 1 is scaled according to the Q value of $M_{\mu\pi}$, then 0.016 ± 0.004 GeV is to be added to these bin edges, i.e., the bin is located within the absolute range $0.422 < M_{\mu\pi} < 0.440$ GeV. The probability that the observed excess is caused by a statistical fluctuation located in the bin which also contains 0.429 GeV, absolute, is $< 10^{-3}$. The probability of the similarly situated excess in (c) being due to a statistical fluctuation at that place is $< 10^{-2}$.

This inspection of the $M_{\mu\pi}$ from the DST indicates fluctuations qualitatively compatible with those from the HLBC. The same conclusion was reached in an earlier analysis,⁵ without a selection on t , with a selection for assigned errors $< 2.5\%$ of $M_{\mu\pi}$ and with the histograms calibrated with respect to the observed m_{Λ^0} by the addition of 0.012 ± 0.002 GeV to $M_{\mu\pi}$ near 0.429 GeV. This latter figure is compatible with 0.016 ± 0.004 GeV, above.

The data in (b) and (c) of Fig. 2 are combined in (b) of Fig. 3. Data from the HLBC are shown again in (a); those individual $M_{\mu\pi}$ have been corrected¹ by adding $0.061(M_{\mu\pi} - m_\mu - m_\pi)$ to each. With the DST, the total data from ν experiments has increased from 70 identified (μ, π) with $M_{\mu\pi} < 0.500$ GeV (calculated) to 1483 values from events with one or more π hypotheses. The probability that the largest excess over the mean of (b) should occur in the bin which corresponds with a significant excess in the previous ν experiments, and be due to statistical fluctuations, is $< 10^{-3}$.

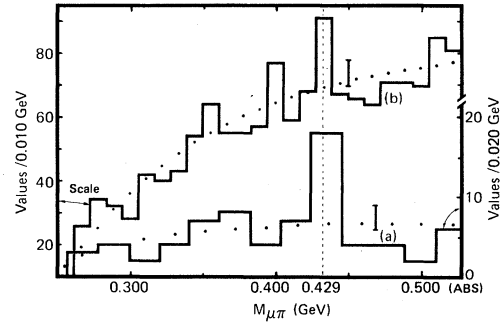


FIG. 3. Histogram (a) is again from the HLBC, (b) is the addition of Fig. 2(b), and (c) from the DST. The estimated errors in the mean absolute mass scale near 0.429 GeV are < 0.004 GeV.

The region around 0.429 GeV will be examined further in Sec. VI, where it will be seen that over a range which includes the next largest excess in (b), three bins to the left of 0.429 GeV, the pattern of fluctuations from the ν experiments corresponds closely with that from K_L^0 decays.

It is important to make clear that each histogram of Fig. 3 results from a series of experiments in a different heavy-liquid bubble chamber separated on average by some six years. The two bubble chambers were served by independent systems of data reduction; however, the same types of installations for the ν beams were used, with the same accelerator, so that the overall ν spectra were almost identical. Before the experiments in Gargamelle had commenced it had been asserted^{1,2} that the probability was entirely negligible that the enhancement in histogram (a) was caused by statistical fluctuations. The information on the DST accords with that assertion. From Fig. 3 alone, the probability is $< 10^{-6}$ that, because of statistical fluctuations, the largest excesses above the smooth means in each histogram should occur at 0.429 GeV. That mass is determined by identically located excesses in K_L^0 observations which, too, occur also in different data with precise mass scales, and are unlikely to be statistical fluctuations. It is untenable to explain these coincidences of enhancements at 0.429 GeV as fortuitous: therefore various possible physical explanations have been tested in detail.

It may be considered, for example, that in other places in (a) and (b) there are also similarities, although of lesser statistical significance than those near 0.429 GeV. Are these types of fluctuations from the smooth mean due to unexpected discontinuities in the ν_μ and $\bar{\nu}_\mu$ spectra? The resultant

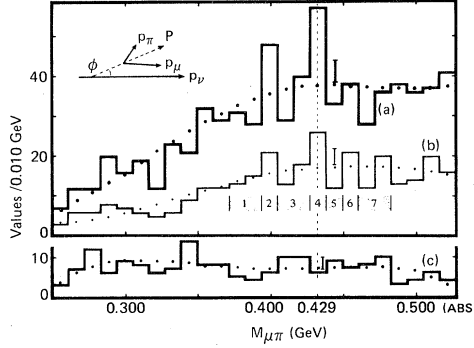


FIG. 4. In the inset ϕ is the inclination of the line of flight of the (μ, π) c.m.s. to the mean direction of the ν beam. The $M_{\mu\pi}$ of Figs. 2(a) and 2(b) are shown in the ranges (a) $0.7 < \cos\phi < 1.0$, (b) $0.95 < \cos\phi < 1.0$, (c) $-1.0 < \cos\phi < 0.7$. The regions 1 to 7 are referred to in Sec. VIII.

momenta of the (μ, π) range from 0.2 to 5 GeV, and they are associated mostly with other particles at the ν vertex in events with different total visible energies. It is kinematically impossible for any fluctuation over a small number of bins in Fig. 3 to reflect the shape of the ν_μ or $\bar{\nu}_\mu$ spectra. From phenomenological considerations and, independently, by kinematical calculation it can be excluded¹ also that the effects at 0.429 GeV are caused by the incorrect (μ, π) assignment of decays of K^0 , Λ^0 , or baryon resonances, or other known processes.

Figure 4 shows a selection of the data of Figs. 2(a) and 2(b) according to the inclination ϕ of the line of flight of the $M_{\mu\pi}$ to the ν -beam direction, 724 of the 904 lines of flight, including those in the enhancement, have $\phi \leq 45^\circ$, 315 have $\phi \leq 18^\circ$. It follows from this diagram that it is untenable to assume that the $M_{\mu\pi}$ are caused by two-body decays of a previously unidentified beam with the same collimation as the ν beam ($\sim 2^\circ$). Before examining further these data from interactions in which there is only one possible combination of (μ, π) , earlier investigations of $M_{\mu\pi}$ distributions from kaon experiments will be described.

IV. MEASUREMENTS OF $M_{\mu\pi}$ FROM K_L^0

The decay $K_L^0 \rightarrow (\mu, \pi, \nu)$, 27% occurs together with other charged modes, including (π^+, π^-, π^0) , 12% and (e, π, ν) , 39%. It is well known that identification of individual μ and π over wide ranges of momentum is impossible. From the frequent decay modes, only the (e, π) , incorrectly as-

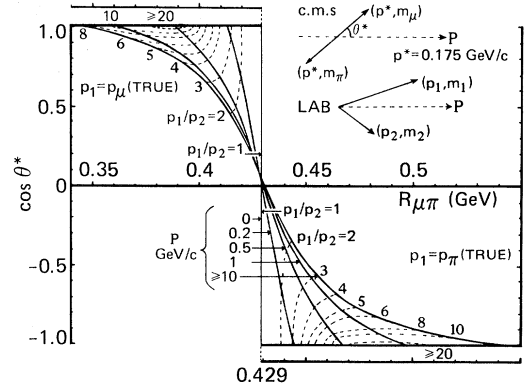


FIG. 5. Distributions of $R_{\mu\pi}$, the invariant mass calculated from the reverse assignment of the tracks of the μ and π from the decay $M_{\mu\pi}^*(0.429) \rightarrow (\mu, \pi)$. In the inset θ^* is the inclination of p^* of the μ , in the c.m.s. of the $M_{\mu\pi}^*$, to the line of flight of that system. The laboratory momenta of the (μ, π) are p_1, p_2 such that $p_1 > p_2$; $\vec{P} = \vec{p}_1 + \vec{p}_2$. If $P=0$, then $p_1=p_2=p^*$ and $R_{\mu\pi} = M_{\mu\pi} = 0.429$ GeV. Except for $\cos\theta^* \sim 0$, if $p_1 = p_\mu > p_\pi$, then $R_{\mu\pi} < M_{\mu\pi}^*$; if $p_1 = p_\pi > p_\mu$, then $R_{\mu\pi} > M_{\mu\pi}^*$.

signed as (μ, π) , can give false values of $M_{\mu\pi}$ near 0.429 GeV: effects from incorrect assignment of contamination by K_S^0 or Λ^0 decays are negligible in that region. In order to extract information from every V^0 , including the significant fraction where the individual particles of the (μ, π) cannot be identified, unconstrained invariant masses were calculated for both (μ, π) assignments for each V^0 , with the assumption that the observed momenta are independent of particle assignment.

Suppose that in the c.m.s. of a correctly assigned (μ, π) the μ momentum is p^* , inclined at θ^* to the line of flight of that system. The invariant mass calculated from the reverse (μ, π) assignment is

$$R_{\mu\pi} = \{ [(p_\mu^2 + m_\pi^2)^{1/2} + (p_\pi^2 + m_\mu^2)^{1/2}]^2 - P^2 \}^{1/2}.$$

Because $m_\mu \neq m_\pi$, the difference $M_{\mu\pi} - R_{\mu\pi}$ will depend on θ^* and on the resultant laboratory momentum $\vec{P} = \vec{p}_\mu + \vec{p}_\pi$. If $p_\mu = p_\pi$, then $R_{\mu\pi} = M_{\mu\pi}$. In other cases the mass $(M_{\mu\pi})_1$, calculated when the particle with the greater momentum is assigned as μ , is $> (M_{\mu\pi})_2$ from the reverse assignment. In this terminology^{1,2} the momenta are $p_1 > p_2$. Except when $\cos\theta^* \sim 0$, \vec{p}_1 is due to the particle with p^* forward with respect to \vec{P} , which generally is not in the direction of the K_L^0 momentum. $R_{\mu\pi}$ calculated from (μ, π) for which the correct assignment gives $M_{\mu\pi}^* = 0.429$ GeV, are shown in Fig. 5 in terms of the $\cos\theta^*$ and P .

Because of momentum limitations of particle identifiers, those decay configurations of $M_{\mu\pi}^*$ with a marked inequality of p_μ and p_π might be detectable in the $R_{\mu\pi}$, $(M_{\mu\pi})_1$, or $(M_{\mu\pi})_2$ distributions from the total data, but not necessarily in $M_{\mu\pi}$ distributions which are restricted to (μ, π) with identified particles. If, for example, decays with $\cos\theta^* > 0$ predominate, then mostly $p_\mu > p_\pi$, and effects of $M_{\mu\pi}^*$ will be mostly in $(M_{\mu\pi})_1$. That this was the actual case was inferred directly from $(M_{\mu\pi})_1$ distributions in which particle identification was not used.

V. ACTUAL $M_{\mu\pi}$ DISTRIBUTIONS FROM K_L^0

In the "X4" experiment^{6,1} in the 0.5-m³ version of the HLBC, the K_L^0 beam was along the axis of a thin-walled vacuum pipe which traversed the working fluid (CF₃Br) so that the (μ, π) emerging from the pipe were almost free from background. Because of the radiation length of ~ 11 cm, (π^+, π^-, π^0) and (e, π, ν) could be separated from (μ, π, ν) . The latter data were considered $> 95\%$ pure: mostly, however, the individual μ and π were not identifiable. Obviously, the pipe obscured the decay vertex and any other phenomena inside, such as π decay in flight. It also caused (μ, π) produced with resultant transverse momenta (p_T) near maximum to have a greater probability of detection than those with $p_T \sim 0$. It was not understood until much later² that this selection enhances the proportion of $M_{\mu\pi}^*$ in the total data. Histogram (a) in Fig. 6 contains $M_{\mu\pi}$ and $R_{\mu\pi}$ from 0.380 to 0.470 GeV. As in the other data in Fig. 6, the mean absolute error in the unconstrained masses is less than the bin width. The scale for (a) was calibrated from reconstruction of (π^+, π^-, π^0) .

Histogram (b) contains both $M_{\mu\pi}$ and $R_{\mu\pi}$ from a K_L^0 experiment^{7,1} in the Brookhaven 14-in. hydrogen bubble chamber (HBC), calibrated with reference to K_S^0 decays. The (μ, π) , (e, π) , (π, π) and (π^-, p) from K_L^0 , K_S^0 , and Λ^0 could not be separated and therefore are calculated for both possible assignments as (μ, π) . Some of the contributions near 0.429 GeV from the true (e, π) have been reduced by discarding V 's with $p_T > 0.1$ GeV/c, and also those in which $p_1/p_2 > 5$. Because

$$E_\nu = (m_{K^0}^2 - M_{\mu\pi}^2) / 2m_{K^0} = p_{T_{\max}},$$

no correctly identified and measured (μ, π) with $M_{\mu\pi} > 0.385$ GeV has $p_T > 0.100$ GeV/c. In this

experiment $\sim 15\%$ of true $(\mu\pi)$ would have $p_1/p_2 > 5$; because $m_\mu \gg m_e$, (e, π) tend to have larger values of p_1/p_2 than (μ, π) . These selections account for the difference in slopes of the means of (a) and (b). Histogram (c) contains $(M_{\mu\pi})_1$ only, from a spark chamber experiment^{8,2} for which the mass scale was calibrated from the high-energy limit of $M_{\pi\pi}$ from (π^+, π^-, π^0) .

According to the accepted understanding of K_L^0 decays, the histograms in Fig. 6 should have smooth means. After thorough investigation it was concluded² that there was negligible probability that the coincidence of the excesses over the means in the bin $0.4275 < M_{\mu\pi} < 0.430$ GeV, in (a), (b), and (c) was of statistical origin. It is excluded, also, that those excesses are due to incorrect assignment of contamination of the K_L^0 by the decay of any known particle, such as K_S^0 or Λ^0 . In the data for (b) and (c), which were obtained without the kinematical influences of a vacuum pipe, it was found that these excesses in $M_{\mu\pi}$ near 0.429 GeV

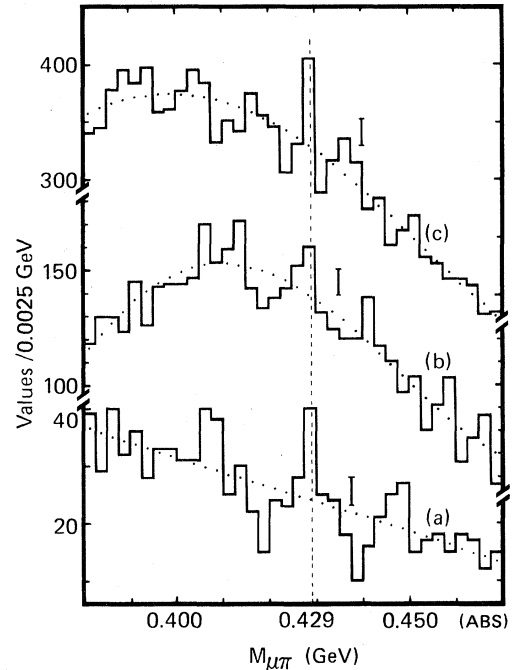


FIG. 6. Histograms from three different experiments on K_L^0 decays. (a) contains both $M_{\mu\pi}$ and $R_{\mu\pi}$ from the 0.5-m³ version of the HLBC, $> 95\%$ are from $K_L^0 \rightarrow (\mu, \pi, \nu)$; (b) contains both $M_{\mu\pi}$ and $R_{\mu\pi}$ from the 14-in. HBC, selected for $p_1/p_2 < 5$ and $p_T < 0.1$ GeV/c; (c) $(M_{\mu\pi})_1$ from a K_L^0 spark-chamber experiment (i.e., in each event the higher momentum track is assigned as μ). The absolute errors in the mean mass scale near 0.429 GeV are < 0.002 GeV.

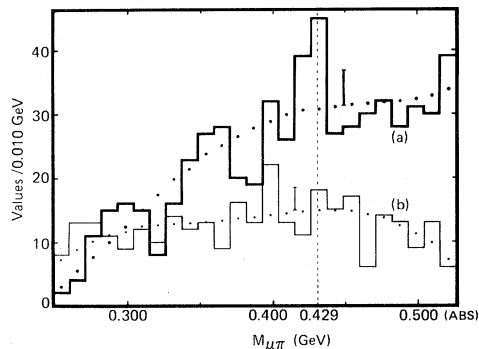


FIG. 7. $M_{\mu\pi}$ from ν and $\bar{\nu}$ events with only one possible (μ, π) , i.e., data of Figs. 2(a) and 2(b). Histogram (a) is for $p_{\mu} > p_{\pi}$; (b) is for $p_{\pi} > p_{\mu}$.

were more pronounced in the $(M_{\mu\pi})_1$ distribution. Therefore, it was inferred that decays of $M_{\mu\pi}^*$ give, predominantly, $p_{\mu} > p_{\pi}$ and hence values of $\cos\theta^* > 0$. In the ν experiments most (μ, π) are correctly assigned so that this inference can be compared directly with the actual situation in the ν interactions.

Histogram (a) in Fig. 7 shows the data from Figs. 2(a) and 2(b) for which $p_{\mu} > p_{\pi}$; it contains 347 values from (μ^-, π^+) and 244 from (μ^+, π^-) , with $M_{\mu\pi} < 0.500$ GeV (calculated). Histogram (b) is for $p_{\pi} > p_{\mu}$ and has 203 (μ^-, π^+) and 110 (μ^+, π^-) . It can be seen that most (μ, π) and, specifically, most which might be attributed to $M_{\mu\pi}^*$, have $p_{\mu} > p_{\pi}$. Therefore, it would be expected that if the $\cos\theta^*$ distribution for $M_{\mu\pi}^*$ produced from K_L^0 is similar to that from ν interactions, the $M_{\mu\pi}^*$ excesses in distributions from K_L^0 would be more pronounced in the data which was assigned as $p_{\mu} > p_{\pi}$ [i.e., $(M_{\mu\pi})_1$]. That had been observed.^{1,2}

VI. COMPARISON OF $M_{\mu\pi}$ FROM DIFFERENT EXPERIMENTS

From an inspection of Figs. 3, 4, and 6, it might be asked whether there are any other systematic fluctuations in the $M_{\mu\pi}$ distributions near 0.429 GeV. Because the data selected in Fig. 4(a) appear to contain all the enhancement near 0.429 GeV in less total data than Figs. 2(a) and 2(b), any other fluctuations associated with $M_{\mu\pi}^*$ are also likely to be enhanced in them. Those data are redrawn in Fig. 8 at (b) in bins of 0.0025 GeV so that they can be compared with (a), which is the K_L^0 observation of Fig. 6(a). The coefficient of correlation,¹ ex-

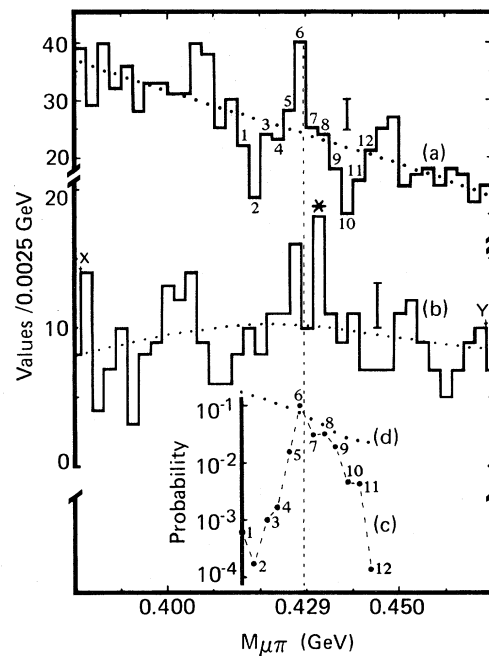


FIG. 8. Comparison of $M_{\mu\pi}$ histograms from $K_L^0 \rightarrow (\mu, \pi, \nu)$ and ν interactions. (a) is the K_L^0 data of Fig. 6(a); (b) is the ν data from Fig. 4(a), redrawn in bins of 0.0025 GeV; the numbered points in (c) show the probability that the range XY of (b) represents the same physical distribution as an equal number of consecutive bins of (a), as the bin with the asterisk is superimposed successively on the numbered bins in (a); (d) shows the result of the same type of comparison between XY and the mean bin heights of (a), shown dotted.

pressed as the probability that the two histograms represent the same mass distribution, has been calculated for successive superpositions of (b) on (a). The points in (c) show the correlations when the part of (b) from X to Y is compared with equal numbers of consecutive bins of (a). The probability of $\sim 6 \times 10^{-4}$ at 1 is calculated when the bin with the asterisk in (b) is aligned with the bin marked 1 in (a): this superposition would have occurred if the mass scale of (b) had not been corrected. The probability that both histograms represent the same distribution is largest (~ 0.1) when the bin with the asterisk is aligned with the bin in (a) containing 0.429 GeV. This position of XY is 0.0035 GeV from the drawn location, where the bin edges are not colinear. As histogram XY is compared in further steps with (a), the probability decreases again to $\sim 10^{-4}$, at 0.0115 GeV from the drawn location.

No compensation has been attempted for the intrinsic difference in phase space or mass calibration of the two sets of data. There is no marked

change in the shape of (c) if X or Y are placed on other bins near those shown. The points in (d) are the correlations, calculated as for (c), when histogram XY is compared with the mean values of (a) instead of the actual bins: It appears that the shape of (c) is not strongly dependent on the mean slope of (a). If the superposition of highest correlation is used to test the mass scale of XY relative to (a), it leads to a correction of 0.0125 ± 0.0025 GeV to be added, compatible with the corrections determined from m_{K^0} and m_{Λ^0} , already described. According to (c), histograms (a) and XY represent best the same mass distribution when their bin edges are aligned within 0.003 GeV of their calibrated mass scales. This result could be due to similar patterns of statistical fluctuations in each $M_{\mu\pi}$ distribution, coincident in absolute value of $M_{\mu\pi}$. It could be due also to a pattern of fluctuations of physical origin near 0.429 GeV which is associated with $M_{\mu\pi}^*$ from both ν interactions and K_L^0 decays. Because the apparent "lobes" at ~ 0.02 to 0.03 GeV above and below 0.429 GeV occur in all data, physical as well as statistical causes of them have been investigated.

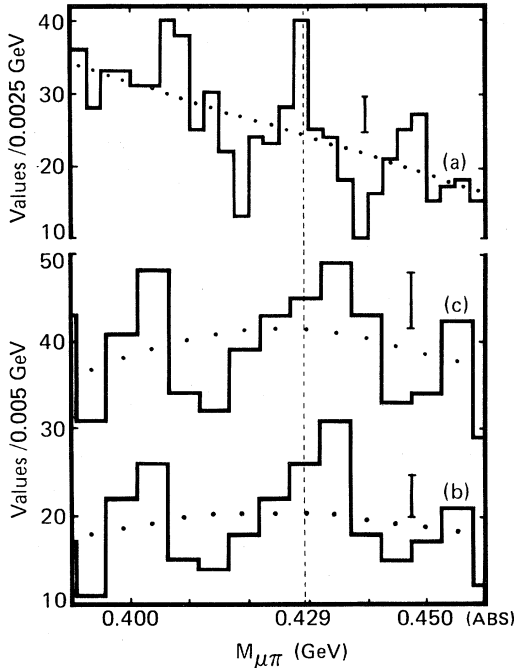


FIG. 9. Histogram (a) is again the K_L^0 data of Fig. 6(a); (b) is the data of Fig. 4(a) in bins of 0.005 GeV, so as to make the lobes more apparent; (c) is the addition of (b) with the $R_{\mu\pi}$ of the data of Fig. 4(a). The bin edges in (b) and (c) have been drawn at their correct absolute masses.

Because $m_\mu \neq m_\pi$, some types of experimental errors could produce fluctuations in $M_{\mu\pi}$ and $R_{\mu\pi}$ distributions near, but not at $M_{\mu\pi}^*(0.429)$. For example, if, due to observational limitations or any other reason, the θ^* of the (μ, π) were distributed preferentially near $\cos\theta^* = \pm 1$, then the $R_{\mu\pi}$ would occur in two regions at nearly equal distances from 0.429 GeV. Those at lower masses would be from $p_\mu > p_\pi$, those at higher masses from $p_\pi > p_\mu$. If, as in the K_L^0 data, $M_{\mu\pi}$ and $R_{\mu\pi}$ could not be identified, any lobes would be separated by a "line" at 0.429 GeV. However, the values of P , the lower limits of detection for p_μ and p_π , and the number of errors in particle assignment required to produce calculated lobes of the amplitude observed are untenable against the experimental facts.

Furthermore, it is shown by experiment in Fig. 9 that while incorrect assignment may contribute to the lobes, it cannot be a major cause of them. Histogram (a) is again for reference from Fig. 6(a); (b) is the data of Fig. 8(b), in bins of 0.005 GeV so as to make the lobes more apparent. The bin edges are in their calibrated positions. Histogram (c) is the combination of (b) with the $R_{\mu\pi}$ distribution, i.e., for each (μ, π) of Fig. 4(a), the invariant mass has been calculated for the correct and incorrect assignments so that (c) is the same type of data as (a). It is considered that on average $> 80\%$ of the true (μ, π) are correctly assigned in (b), therefore it might be expected that the inclusion in (c) of the $R_{\mu\pi}$ could increase some fivefold the effects due to wrong assignment. The increase of the lobes with respect to (b) is $\ll 5$ times: therefore those in (b) cannot be due largely to assignment errors of the (μ, π) , randomly distributed in $M_{\mu\pi}$.

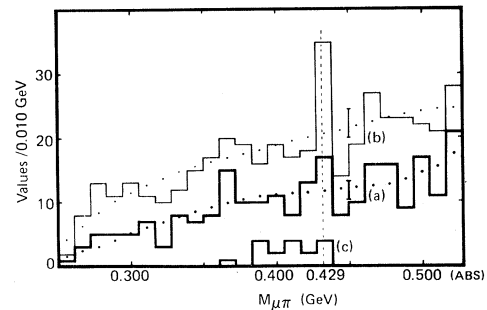


FIG. 10. Histogram (a) contains the $M_{\mu\pi}$ of Fig. 7(a) for which $p_{\mu^+} > p_{\pi^-}$, i.e., it includes values from $\bar{M}_{\mu\pi}^*$; (b) shows the addition of (a) with $R_{\mu\pi}$ of the $p_{\pi^+} > p_{\mu^-}$ of Fig. 7(b). Any (μ, π) which is reverse assigned in the scanning, but which is actually $p_{\mu^+} > p_{\pi^-}$, is thus included in (b). The data in (c) show the original $M_{\mu\pi}$ of Fig. 7(b), which have $R_{\mu\pi}$ in the bin in (b) containing 0.429 GeV.

In searching generally for effects from assignment errors, each $R_{\mu\pi}$ distribution from the ν data has been compared with various selections of $M_{\mu\pi}$. Only one small group of possibly reversed assignments has been found: it does not cause a lobelike distribution. Histogram (a) in Fig. 10 contains those $M_{\mu\pi}$ of Fig. 7(a) with $p_{\mu^+} > p_{\pi^-}$, which would include $\overline{M}_{\mu\pi}^*$ decays. If any of these (μ, π) were reverse assigned in the original data, they would be in the selection with $p_{\pi^+} > p_{\mu^-}$. There is an excess in the bin containing 0.429 GeV in the $R_{\mu\pi}$ of this selection: the result of adding these $R_{\mu\pi}$ to (a) is shown in (b). The probability that the excess above the mean in the bin with 0.429 GeV would be due to statistical fluctuations at that particular place is $< 10^{-4}$. The part of this excess in the $R_{\mu\pi}$ distribution would be caused if nine of the (μ^-, π^+) with $p_{\pi^+} > p_{\mu^-}$ in the data were actually (π^-, μ^+) with $p_{\mu^+} > p_{\pi^-}$. Such an error would be unimportant in the overall analyses; however, it would mean that nine $\overline{M}_{\mu\pi}^*$ should be added to the bin containing 0.429 GeV in each of Figs. 7(a) and 10(a), almost doubling the excess which can be attributed to $\overline{M}_{\mu\pi}^*$ in the latter.

A possible cause of the effect in histogram (b) could be that μ^+ occur less frequently than μ^- in the ν experiments. All scanners know that ambiguity of μ and π of opposite charge is resolved correctly, more often by the assignment of the negative track as μ . If the overall cross section of (μ^+, π^-) production as a function of $M_{\mu\pi}$ were smooth, any errors of assignment caused by this logical scanning preference would be a constant fraction of the $M_{\mu\pi}$. However, if the cross section varied in such a way as to enhance the occurrence of (μ, π) with $p_{\mu^+} > p_{\pi^-}$ at a particular $M_{\mu\pi}$, e.g., due to $\overline{M}_{\mu\pi}^*$ production, the result in (b) could arise. Such an explanation accords with HLBC observations, where the data were from ν interactions with some $\bar{\nu}$ contamination and were restricted to "identified" (μ, π) . Of the six values¹ of $M_{\mu\pi} < 0.500$ GeV from (μ^+, π^-) , five were compatible with $\overline{M}_{\mu\pi}^*$. If a uniform distribution of $M_{\mu\pi}$ were expected, then the probability is $< 10^{-3}$ that the accumulation of five values at $\overline{M}_{\mu\pi}^*$ was due to a statistical fluctuation. A more likely explanation is, as for Fig. 7(b), that there is an enhanced number of (μ^+, π^-) from $\overline{M}_{\mu\pi}^*$ production. As can be seen in (c), the distribution of the original $M_{\mu\pi}$ of all the $R_{\mu\pi}$ in the bin at 0.429 GeV in (b) does not resemble the lobe at lower mass. From Fig. 5 it can be seen that for $p_{\pi} > p_{\mu}$ (true), $M_{\mu\pi} < R_{\mu\pi}$.

From these and other tests of hypotheses for

lobe production, including effects of π decay in flight and also of assignment errors combined with range-energy momentum determinations, no quantitative explanation has been found for the lobes of Fig. 9 which does not invoke some otherwise unobserved physical phenomena. Nevertheless, it is unlikely that the lobes are due to statistical fluctuations.

VII. EFFECTS OF EXPERIMENTAL LIMITATIONS

In the ν experiments the assigned r.m.s. mass errors near 0.4 GeV are in the range 0.5 to 10 %, most are $< 3\%$. The nature of the error distribution and the stability of calibration of the mean-mass measurements determine the detectability of any patterns in the $M_{\mu\pi}$ distributions: it can be inferred from Figs. 6, 8, and 9 that sporadic changes of $\sim 1\%$ in the calibration of the mean $M_{\mu\pi}$ values would almost obliterate departures from smooth near 0.429 GeV, which were of physical origin. In all $M_{\mu\pi}$ distributions which I have examined, such departures are statistically significant whenever there has been a reproducibility in mean unconstrained mass measurement $\lesssim 1\%$ throughout data acquisition.

In bubble chambers, the long-term reproducibility of the mean-mass scale, as distinct from the mass resolution at any given stage in the experiment, is assured by maintaining a constant magnetic field. No such single parameter dominates mass scale reproducibility in spark chambers. Their intrinsic data-gathering possibilities cannot be used to advantage for the present study unless associated with adequate stability of unconstrained mass measurement. The decay $K_S^0 \rightarrow (\pi, \pi)$ and the slope and end point of the higher values of $M_{\pi\pi}$ from $K_{\pi 3}^0$ are useful references; erroneous (μ, π) assignment of them gives calculable features near 0.48 and 0.35 GeV, respectively, which can be monitored continuously in $M_{\mu\pi}$ distributions. Contamination from Λ^0 cannot produce a readily distinguishable discontinuity. It is asymmetrical with respect to charge assignment.

Other important differences between K_L^0 experiments are the ways in which observations of phase spaces are restricted, either due to impossibility to detect one or other member of the V^0 from some kinematical configurations of the decays, or because of the restricted momentum ranges over which particles can be identified. In bubble chambers, almost all regions of Dalitz plots of the

$K_{\mu 3}^0$ c.m.s. are accessible, but the confusion in locating the data points because of the effects of the well-known quadratic ambiguity is unavoidable: the ν associated with the (μ, π) is undetectable. Independently of Dalitz plots, all the phase space for $\cos\theta^*$ is accessible.

In the K_L^0 spark-chamber experiment of Chien *et al.*,⁸ almost all decay configurations were detectable. After calibration, and by not restricting the data to those (μ, π) which had been signified as such by the particle identifiers, I found that the effects of $M_{\mu\pi}^*(0.429)$ were readily observable² for $\cos\theta^* > 0$ and for $p_T \sim p_{T \max}$. For $\cos\theta^* \sim 0$ which, because of the momentum restrictions for particle identification is the region most frequently occupied by identified (μ, π) , the effects were of little statistical significance. The experiments of Bisi *et al.*³ and Clark *et al.*⁴ were made in installations designed for the study of those decay configurations of K_S^0 for which $p_\mu \sim p_\pi$ and for which, of course, there is most phase space in the laboratory. When such installations are used to study $M_{\mu\pi}$ near 0.429 GeV, they have the merit of a known calibration with respect to m_{K^0} ; however, they select, mostly, (μ, π) for which $\cos\theta^* \sim 0$ and $p_T \sim 0$, for which there is little production of $M_{\mu\pi}^*(0.429)$.

Donaldson *et al.*, reported⁹ that with a resolution of ± 3 MeV in a spark-chamber experiment yielding 1.6×10^6 decays of $K_L^0 \rightarrow (\mu, \pi, \nu)$, no departures from smooth were seen anywhere in the $M_{\mu\pi}$ distribution and there was no excess of events around 420 MeV. In order to assess the potential of their experiment for the study of $M_{\mu\pi}^*$, a demonstration of the constancy of the absolute mass calibration throughout all the data acquisition is necessary. Such information is not included in their report. In the same volume in which 1.6×10^6 (μ, π, ν) were observed, there would have been 0.7×10^6 (π^+, π^-, π^0) and, in the absence of a regenerator, some 1.2×10^4 (π^+, π^-) : the total $K_S^0 \rightarrow (\pi^+, \pi^-)$ data is especially valuable as an indicator of long-term constancy of mass calibration. The nature of the overall $M_{\mu\pi}$ distribution in Fig. 24 of Donaldson *et al.* does not *per se* exclude evidence of $M_{\mu\pi}^*(0.429)$ elsewhere in their observations. The overall spark-chamber data from which the present Fig. 6(c) is obtained would show a comparable $M_{\mu\pi}$ distribution near 0.429 GeV, if displayed in the same manner. Similarly, the full range of the X4 data, which includes those in Fig. 6(a) is, in larger bins, an excellent fit to a smooth phase space from a Monte Carlo calculation.

In a hypothetically ideal experiment in which all decay configurations and all three of the (μ, π, ν) were detected, so that there was no quadratic ambiguity, the Dalitz plot of (T_μ, T_π) in the $K_{\mu 3}^0$ c.m.s., used by Donaldson *et al.*, would have changes in density due to $M_{\mu\pi}^*(0.429)$ along the line $T_\mu + T_\pi = M_{\mu\pi}^* - m_\mu - m_\pi$. An above-average density of data points would be expected on that line near the higher boundary of T_μ . Another² Dalitz plot for such an investigation is of $(T_\mu, M_{\mu\pi})$: T_μ is linear in the cosine of the angle between the μ and ν directions in the $M_{\mu\pi}$ c.m.s. Given sufficient stability of the mass scale, the quantity of data available from an experiment of the type of Donaldson *et al.* would permit searches for $M_{\mu\pi}^*$ in intervals smaller than in the Dalitz plot of their Fig. 16, and with many different possibilities of cuts. However, because of the limitations in p_1/p_2 and therefore $\cos\theta^*$, caused by particle identification, and the double degree of ambiguity which gives four locations of each (μ, π) in a Dalitz plot if particle identifiers are not used, it would be informative first to investigate $M_{\mu\pi}$ and $R_{\mu\pi}$ from (μ, π) assignments of all V^0 , with selections in p_1 , p_2 and p_T , following the principles already described.

VIII. DISTRIBUTION OF $\cos\theta^*$ NEAR 0.429 GeV

In Fig. 11(a)–11(d), the data of Fig. 4(a) are selected into four equal intervals in $\cos\theta^*$. The diagram accords with the already-deduced predominance of $\cos\theta^* > 0$. Qualitatively it seems that the lobes of Fig. 9 tend to be contributed by the (μ, π) with $-0.5 < \cos\theta^* < 0.5$; this accords with the deduction that they are not mostly $R_{\mu\pi}$ from $M_{\mu\pi}^*(0.429)$. If the lobes were formed by $R_{\mu\pi}$,

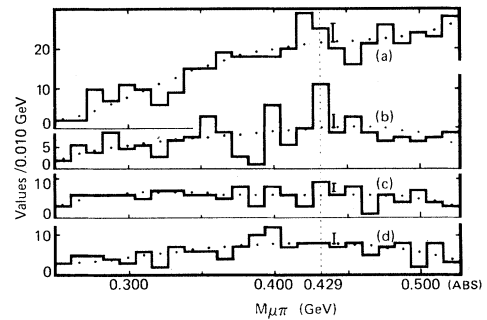


FIG. 11. Histograms of all the $M_{\mu\pi}$ of Fig. 4, selected according to $\cos\theta^*$ of the (μ, π) . (a) $0.5 < \cos\theta^* < 1$; (b) $0 < \cos\theta^* < 0.5$; (c) $-0.5 < \cos\theta^* < 0$; (d) $-1 < \cos\theta^* < -0.5$.

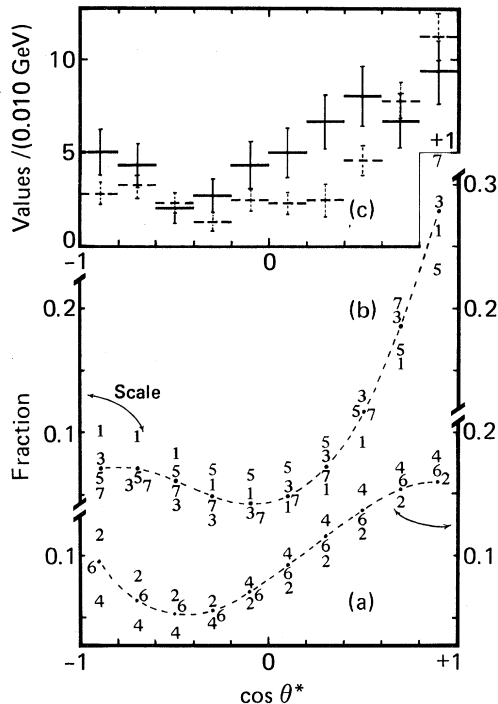


FIG. 12. The numbers show the positions of the polynomial means of the $\cos\theta^*$ distributions in the seven regions of $M_{\mu\pi}$ shown in Fig. 4. The points in (a) are for the regions of “enhancement” (4) and the “lobes” (2,6), the ordinate is the fraction of events in each region in intervals of 0.2 in $\cos\theta^*$. The curve connects the means of all those data ($\chi^2=4.9$). The points in (b) are for the regions (1,3,5,7), adjacent to the lobes and enhancement and the curve connects the means of all those data ($\chi^2=3.1$). The solid lines in (c) show the actual $\cos\theta^*$ distribution of the $M_{\mu\pi}$ in the “average bin” of 0.010 GeV of the regions 2,4,6 of (a); the dashed bars refer, correspondingly, to the “average bin” of regions 1,3,5,7 of (b), in intervals of 0.2 in $\cos\theta^*$.

their major contributions would come from the regions $\cos\theta^* \sim \pm 1$.

The $\cos\theta^*$ composition of the data of Fig. 4(a) and (c) near 0.429 GeV has been examined in each of the contiguous regions of $M_{\mu\pi}$, numbered 1 to 7 in that figure; they are either of 1 or 2 bins, region (4) is the “enhancement,” regions (2,6) are the “lobes.” The regions have, respectively, 68, 54, 89, 63, 42, 45, and 82 events. For convenience of inspection a third-degree polynomial mean in $\cos\theta^*$ has been least-squares fitted in each region to the fraction of events in each of the 10 equal intervals of 0.2 in $\cos\theta^*$. There is no intended physical significance in the choice of mean, the results obtained are similar for second and fourth degree. The means of each region are shown by the num-

bers in Fig. 12: (a) is for the enhancement and lobes, (b) is for the adjacent regions (1,3,5,7). The fits of the distribution of the actual data to the sets of numbered points are in the range $1.9 < \chi^2 < 6.8$, i.e., typically 80%.

The calculated means of the regions in (a) are similar, as are also those in (b). However, the means of all the data in each of (a) and (b), shown dashed, appear significantly different: The probability is $\sim 5 \times 10^{-4}$ that the distribution of all the observed $\cos\theta^*$ of (a) might be a statistical fluctuation of a distribution in which the dashed mean of (b) is expected. If this difference were physical, as seems likely, then it would follow that the $\cos\theta^*$ distribution varies markedly over changes in $M_{\mu\pi} \sim 0.01$ GeV. That possibility accords with the fluctuations in $(M_{\mu\pi})_1$ and $(M_{\mu\pi})_2$ in K_L^0 observations. As information, the solid bars in (c) in Fig. 12 show the distribution of $\cos\theta^*$ in terms of the $M_{\mu\pi}$ in the “average bin” of 0.010 GeV in the regions 2, 4, 6 of (a), (three bins, 162 values); the dashed bars refer, correspondingly, to the average bin of the regions 1, 3, 5, 7 of (b), (seven bins, 281 values). Until the cause of the lobes near 0.429 GeV is understood, it is not meaningful to estimate a $\cos\theta^*$ distribution for the decay of $M_{\mu\pi}^*(0.429)$ from any differences of such diagrams.

IX. INSPECTION OF $M_{\mu\gamma}$

In the 1.1-m³ HLBC ν experiments the unconstrained invariant masses of muon-single- γ combinations were calculated¹⁰ from interactions in propane of the type

$$\nu_\mu + N \rightarrow \mu^- + n(\gamma) + \dots + N'$$

and

$$\bar{\nu}_\mu + N \rightarrow \mu^+ + n(\gamma) + \dots + N',$$

where n is 1, 2, or 3. Possible effects due to π^0 production were eliminated by rejecting any $M_{\mu\gamma}$ if the γ , when paired with any other from the same vertex, had a probability $> 1\%$ of being $\pi^0 \rightarrow 2\gamma$. The distribution of the remaining $M_{\mu\gamma}$ from (μ^-, γ) and $M_{\mu\gamma}$ from (μ^+, γ) , in which the same μ can contribute up to three different values, is shown in histogram (a) in Fig. 13. The $M_{\mu\gamma}$ mass scale cannot be calibrated as directly as that of $M_{\mu\pi}$. The mean value of $M_{\mu\gamma}$ due to $\pi^0 \rightarrow 2\gamma$ was 0.134 ± 0.002 GeV. From this and the observed value of m_{Λ^0} , the error in the mean calculated $M_{\mu\gamma}$ near 0.429 GeV was estimated at < 0.010 GeV, i.e., less than half the bin width of (a).

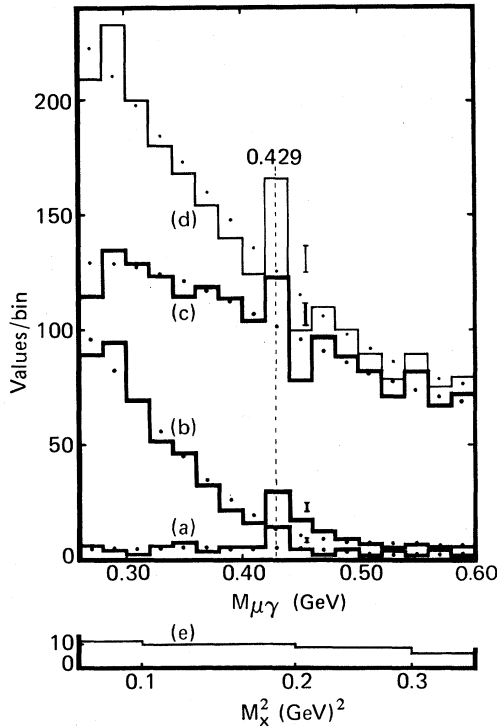


FIG. 13. Histograms of $M_{\mu\gamma}$ (bins 0.020 GeV). (a) From the ν experiments in the HLBC; (b) from a muon-bremsstrahlung experiment of Liberman *et al.*; (c) from ν_μ and $\bar{\nu}_\mu$ experiments in C_3H_8 on the DST; (d) combination of (a), (b), and (c). The estimated absolute errors in $M_{\mu\gamma}$ near 0.429 GeV are <0.010 GeV. Histogram (e) [bins 0.1 GeV^2] is the distribution of M_{X^2} read from Figs. 3(a) and 3(b) of the paper by Gittleston *et al.*, on the interaction $\mu + p \rightarrow p + X$, without identification of X . The stated errors in M_{X^2} are ~ 0.5 GeV^2 , to be compared with the total range of ~ 0.3 GeV^2 of this figure.

Histogram (b) shows the $M_{\mu\gamma}$ distribution from the muon-bremsstrahlung spark-chamber experiment of Liberman *et al.*, who studied^{11,12,10} the interaction $\mu + N \rightarrow \mu + \gamma + N'$ from a muon beam of $9 < p_\mu < 13$ GeV/c on a carbon plate target. Because of the correspondence of the excesses in (a) and (b), the fact that they were contributed to by (μ^-, γ) and (μ^+, γ) , that it was unlikely the coincidences were due to statistical fluctuations, and the evidence for the decay of $M_{\mu\pi}^*(0.429)$, I consider that there exists a charged lepton and antilepton with a similar mass. It is produced in μ and ν_μ interactions with nucleons and has decay modes $M_{\mu\gamma}^* \rightarrow (\mu^-, \gamma)$ and $\bar{M}_{\mu\gamma}^* \rightarrow (\mu^+, \gamma)$.

Values of $M_{\mu\gamma}$ have been calculated for ν vertices in propane classified on the DST with one "good" μ and up to 3γ : they are shown in histo-

gram (c). Because of its radiation length of ~ 1 m, errors of reconstruction and measurement of γ momenta are smaller in propane than in freon. Only the propane data from the DST were used for comparison with those of the HLBC. In an earlier analysis⁵ of those (γ, γ) on the DST likely to be from $\pi^0 \rightarrow 2\gamma$, the mean $M_{\gamma\gamma}$ was in the range $0.131 < M_{\gamma\gamma} < 0.135$ GeV. From this and the observed correction for $M_{\pi\pi}$ near m_{K^0} , it was estimated that the error in the mean calculated $M_{\mu\gamma}$ near 0.429 GeV is $\lesssim 0.010$ GeV. According to other calibrations it is likely that the corrections to $M_{\mu\gamma}$ from the HLBC and DST have the same sign.

The combined data of Figs. 13(a)–13(c) are shown in histogram (d). The probability that the bin containing 0.429 GeV is due to a statistical fluctuation about the mean of all the data is 3×10^{-4} if that bin is included in the mean, and $< 10^{-5}$ if that bin is excluded. The probability that, if the mean values were the expected distribution, statistical fluctuations in the independent experiments would produce the observed coincidence of excesses is $< 10^{-6}$.

This inspection of the $M_{\mu\gamma}$ from the DST shows an effect in accord with that already published. It appears, also from (c) and from histograms with narrower bins, that there may be a pattern of fluctuations in regions near 0.429 GeV, as there is in the $M_{\mu\pi}$ histograms. This possibility is being studied.

From a study of the process $\mu + p \rightarrow p + X$ in interactions of 5.8 and 7.2 GeV μ beams in a liquid-hydrogen target, Gittleston *et al.* reported¹³ that there was no evidence for the production of excited muons in the mass range 0.0 to 2.0 GeV. Their distribution of M_{X^2} , read from their Figs. 3(a) and 3(b), over the range of $M_{\mu\gamma}$ of Fig. 13, is shown at (e). That portion of their data, in bins of 0.1 GeV^2 , comprises some 30 values of M_{X^2} with experimental errors of ± 0.5 GeV^2 . It can be compared with the 70 $M_{\mu\gamma}$ values from the HLBC ν experiment, 508 $M_{\mu\gamma}$ from identified (μ, γ) interactions from the experiment of Drickey *et al.*, and some 2293 total values of $M_{\mu\gamma}$ in (d) over the range in $M_{\mu\gamma}$ in the figure, with estimated mass errors near 0.429 GeV of ± 0.01 GeV. In the "missing-mass" experiment the X were not identified. Even with the unjustifiable assumption that all the M_{X^2} in (e) were actually $M_{\mu\gamma}^2$, those observations would not be able to detect an excited muon which caused the enhancements in the $M_{\mu\gamma}$ distributions in Fig. 13.

X. PRODUCTION AND DECAY

In the HLBC ν data with identified π , 14 ± 4 of the 70 events with $M_{\mu\pi}^* < 0.500$ GeV could be attributed to $M_{\mu\pi}^*$ and the lobes. Of the 50 events with $p_{\mu} > p_{\pi}$, the corresponding attribution was 11 ± 4 . This latter figure is compatible with 70^{+30}_{-20} of the 591 events from the DST with $M_{\mu\pi}^* < 0.500$ GeV and $p_{\mu} > p_{\pi}$ in Fig. 7, which could be attributed to $M_{\mu\pi}^*$ and lobes. Because a criterion of (μ, π) selection from the DST is a π hypothesis, the selection $p_{\pi^+} > p_{\mu^-}$ will include more protons assigned as π than the selection $p_{\mu^-} > p_{\pi^+}$ and therefore, is less directly comparable with HLBC data.

It was concluded from Fig. 4 that the $M_{\mu\pi}^*$ in ν experiments are not explicable as the two-body decay of a beam of particles with the same collimation as the ν beam. Since the maximum p_T of the $M_{\mu\pi}^*$ in the K_L^0 observations seem as expected from $K_L^0 \rightarrow (M_{\mu\pi}^*, \nu)$, a similar conclusion obtains. From the average characteristics of the particle tracks in the X4 and ν experiments, it was considered that most of the assigned (μ, π) were actually such: it is logical however, to ask whether this is true, specifically, for those attributed to the decay of $M_{\mu\pi}^*(0.429)$.

If the mass of either the apparent “ μ ” or “ π ” from $M_{\mu\pi}^*(0.429)$ were 0.020 GeV different from m_{μ} or m_{π} , the estimated broadening of the enhancement because of the inappropriate invariant-mass calculations would be ~ 0.005 GeV, which would have been noticeable in the HBC and spark-chamber data. The corresponding change in the maximum p_T in K_L^0 decays would be ~ 0.040 GeV. Such a discrepancy with the observed p_T of (μ, π) with $M_{\mu\pi}^* \sim 0.429$ GeV, would have been noticed. There are no significant discrepancies in the kinematics and no unusual features of the “ (μ, π) ” were found in the scanning in the heavy-liquid bubble chambers. Therefore, it is assumed that the “ (μ, π) ” are actually such.

No evidence of flight paths could be found on the HLBC film. The widths of the $M_{\mu\pi}^*$ enhancements from the DST for production in propane and in freon are similar; they are similar also to those in the enhancements from K_S^0 in Fig. 1. If the $M_{\mu\pi}^*$ decayed mostly in the nucleus where it was produced, then because of the possibility of π scattering in that nucleus, the enhancements from the ν experiments might be noticeably broader than the enhancements from K_S^0 , and from $M_{\mu\pi}^*$ from K_L^0 . There are no indications that their widths are

due to other than experimental errors. Assuming the natural width of $M_{\mu\pi}^*(0.429)$ is < 0.005 GeV and the flight path < 1 mm, its lifetime is in the range 10^{-22} to 10^{-12} sec.

The experimental difficulties in measurements associated with the (μ, γ) vertex are clearly greater than at the (μ, π) vertex. At this stage numerical estimates of the effects due to differences in the γ detection and measuring efficiencies in the HLBC and Gargamelle have not been made, so that no information is available which supersedes any of that previously published.¹⁰

No restriction was imposed on the $M_{\mu\pi}^*$ which are produced in interactions (1,2) and in which there may be one or more π of charge opposite to that in the (μ, π) . From Fig. 2 it appears that $M_{\mu\pi}^*$ can be produced in association with π of the same charge as that in the (μ, π) . The γ 's in the data from the HLBC were restricted¹⁰ to those which were unlikely to be associated with π^0 . However, no restrictions other than those described in Sec. IX have been used with the DST. Thus no exclusion to the production of $M_{\mu\pi}^*$ or $M_{\mu\gamma}^*$ in association with other particles in ν interactions has been noted.

No indication of the process $M_{\mu\gamma}^* \rightarrow (\mu, 2\gamma)$ was detectable. It is estimated that if it exists at all, it has $< 50\%$ of the rate of the (μ, γ) decay. Decays of the types $M_{\mu\pi}^* \rightarrow (\mu, \pi, U)$ or $M_{\mu\gamma}^* \rightarrow (\mu, \gamma, U)$ or (μ, U) , where U is some hitherto unobserved light neutral particle, e.g., as proposed by Fayet,¹⁴ would be unlikely to be noticed unless some property of the U attracted the attention of the scanners. From the HLBC observations it is estimated that such decays would not have caused significant features in the invariant-mass distributions unless their rates were \sim twice those of the observed decays of $M_{\mu\pi}^*$ and $M_{\mu\gamma}^*$. Under certain conditions, a three-body decay involving a light neutral can be another model for a production of lobes; it has a kinematical resemblance to the effects of π decay in flight.

XI. CONCLUSION

According to the earlier analyses of $M_{\mu\pi}^*$ distributions from the HLBC ν observations and from K_L^0 , it was to be expected that the information on the DST would be compatible with the decay of a particle of narrow width and a mass of 0.429 ± 0.002 GeV absolute.

(a) Within experimental errors of ± 0.004 GeV, the location of the largest fluctuation above the

mean of that part of the distribution from the DST for which $M_{\mu\pi} < m_{K^0}$ is at 0.429 GeV absolute.

(b) This enhancement has a width comparable with that observed for the decay $K_S^0 \rightarrow (\pi, \pi)$ in the same experiments.

(c) It is contributed to by both (μ^-, π^+) and (μ^+, π^-) .

(d) It is associated with (μ, π) for which, mostly, $p_\mu > p_\pi$.

(e) The shape of the $M_{\mu\pi}$ distribution from the ν experiments, for ~ 0.03 GeV above and below 0.429 GeV is similar to that from K_L^0 experiments and similarly located in absolute mass.

It was asserted also before the Gargamelle experiments commenced that it was untenable to discount the original observations and their occurrence in both ν and K_L^0 experiments, as statistical fluctuations in the data then available. It is clear that assertion was justified. The information on the DST accords in detail with the proposition for which there was already confirmation² in 1973, viz., that in ν interactions, as in decays of K_L^0 , short-lived neutral particles and antiparticles are produced. They decay by the processes $M_{\mu\pi}^*(0.429) \rightarrow (\mu^-, \pi^+)$ and $\bar{M}_{\mu\pi}^*(0.429) \rightarrow (\mu^+, \pi^-)$. From the DST their mass width is less than the experimental resolution, i.e., $\lesssim 0.010$ GeV; from the K_L^0 observations it is likely to be < 0.0025 GeV.

Because each individual μ and π cannot be identified, the possibility that this proposition may have been based on the erroneous (μ, π) assignment of some already known phenomenon has been investigated exhaustively. The risk of such an accident is limited by the observations that the (μ, π) attributed to $M_{\mu\pi}^*(0.429)$ (i) occur in K_L^0 decays and in ν interactions with nucleons, (ii) have maximum transverse momenta which are indistinguishable from that of (μ, π) from $K_L^0 \rightarrow (\mu, \pi, \nu)$, (iii) exhibit similar features in distributions from both

(μ^-, π^+) and (μ^+, π^-) , and (iv) have no visible flight paths in ν interactions. No established process such as the decay of K_S^0 or Λ^0 , erroneously assigned as (μ, π) , can satisfy these constraints. Nor is any other explanation of them feasible unless it invokes hitherto unreported physical effects.

It is also highly untenable to discount the similarity of the $M_{\mu\gamma}$ distribution from the DST to the previously reported results, and those results, as due to statistical fluctuations. The distributions accord with the proposition of the production of a short-lived charged particle and antiparticle which decay $M_{\mu\gamma}^* \rightarrow (\mu^-, \gamma)$ and $\bar{M}_{\mu\gamma}^* \rightarrow (\mu^+, \gamma)$, with a mass within 0.010 GeV of $M_{\mu\pi}^*(0.429)$ and mass width < 0.020 GeV. No possible assignment errors are known which could account for the observations: the γ 's and the μ 's were not seen to be different from others of the $M_{\mu\gamma}$ distributions.

Experimental circumstances alone have caused the investigations reported here to be confined to $M_{\mu\pi}^*(0.429)$ and the $M_{\mu\gamma}^*$ of similar mass: none of these studies excludes the possibility that there may be $M_{\mu\pi}^*$ and $M_{\mu\gamma}^*$ with other masses. However, acceptance of even their existence at 0.429 GeV requires fundamental changes in the present understanding of neutrinos, muons, and kaons.

ACKNOWLEDGMENTS

My warmest thanks are due, in this report, to A. Rousset, J. B. Pattison, and C. Matteuzzi, who introduced me to the system of the DST; to H. Cabel and J. Semmens for meticulous assistance with data reduction. I remain deeply indebted to my colleagues and fellow members of the former N.P.A. division of CERN and to the experimental groups whom I have acknowledged in previous papers and who made available the observations for these analyses.

¹C. A. Ramm, Nature **227**, 1323 (1970).

²C. A. Ramm, Nuovo Cimento **16A**, 47 (1973).

³V. Bisi, M. Cullen, P. Darriulat, C. Grosso, M. I. Ferrero, E. Radermacher, C. Rubbia, D. Shambroom, A. Staude, and K. Tittel, Report No. CERN, D.Ph 1, 1970 (unpublished).

⁴A. R. Clark, T. Elioff, R. C. Field, H. J. Frisch, R. P. Johnson, L. T. Kerth, G. Shen, and W. A. Wenzel, Nature **237**, 388 (1972).

⁵C. A. Ramm, University of Melbourne report, 1977 (unpublished).

⁶G. R. Evans, M. Golden, J. Muir, K. J. Peach, L. A.

Budagov, H. Hopkins, W. Krenz, F. Nezzrick, and R. G. Worthington, Phys. Rev. Lett. **23**, 427 (1969).

⁷H. W. K. Hopkins, T. C. Bacon, and F. R. Eisler, Phys. Rev. Lett. **28B**, 215 (1968).

⁸C. Y. Chien, B. Cox, L. Ettlinger, L. Resvanis, R. A. Zdanis, E. Dally, P. Innocenti, E. Seppi, C. D. Buchanan, D. J. Drickey, F. D. Rudnick, P. F. Shephard, D. H. Stork, and H. K. Ticho, Phys. Lett. **33B**, 627 (1970).

⁹G. Donaldson, D. Fryerberger, D. Hitlin, J. Liu, B. Meyer, R. Piccioni, A. Rothenberg, D. Uggla, S. Wojcicki, and D. Dorfan, Phys. Rev. D **2**, 2960

- (1974).
- ¹⁰C. A. Ramm, *Nature* 230, 145 (1971).
- ¹¹A. D. Liberman, C. M. Hoffman, E. Engels, D. C. Imrie, P. G. Innocenti, R. Wilson, C. Zajde, W. A. Blanpied, D. G. Stairs, and D. J. Drickey, *Phys. Rev. Lett.* 22, 663 (1969).
- ¹²A. D. Liberman, thesis, Harvard University, 1969 (unpublished).
- ¹³H. Gittleson, T. Kirk, M. Murtagh, M. J. Tannenbaum, A. Entenberg, H. Jöstlein, L. Kostoulas, A. C. Melissinos, L. M. Lederman, P. Limon, M. May, P. Rapp, J. Sculli, T. White, and T. Yamanouchi, *Phys. Rev. D* 10, 1379 (1974).
- ¹⁴P. Fayet, *Nucl. Phys.* B187, 184 (1981).